

Axion minicluster streams in the Solar neighbourhood

Ciaran A. J. O'Hare,^a Giovanni Pierobon^{b*} and Javier Redondo^{c,d}

^a*School of Physics, The University of Sydney, NSW 2006 Camperdown, Sydney, Australia*

^b*School of Physics, The University of New South Wales, NSW 2052 Kensington, Sydney, Australia*

^c*CAPA & Departamento de Fisica Teorica, Universidad de Zaragoza, 50009 Zaragoza, Spain*

^d*Max-Planck-Institut für Physik (Werner-Heisenberg-Institut), Föhringer Ring 6, 80805 München, Germany*

E-mail: g.pierobon@unsw.edu.au

The axion, introduced by Peccei and Quinn to solve the strong CP problem, is a compelling candidate for explaining the mysterious nature of dark matter in the universe. In the post-inflationary scenario of axion dark matter, the matter distribution on small scales is populated by sub-parsec, planetary-mass halos known as axion miniclusters. In this contribution, we estimate the mass typically lost by axion miniclusters and explore the resulting formation of tidal streams that could surround our galaxy. Additionally, we assess the detectability of axions in the solar neighborhood and predict the typical signal that would be observed in haloscope experiments targeting the post-inflationary scenario.

*2nd General Meeting of COST Action COSMIC WISPerS (CA21106)
3–6 September 2024
Istinye University, Istanbul, Turkey*

*Speaker

1. Introduction

The QCD axion of Peccei & Quinn, originally postulated to solve the strong CP puzzle [1–3], is one of the most well motivated candidates for the observed dark matter (DM) in the Universe. In the recent years, an expanding campaign of state-of-the-art experiments have been probing axions as dark matter and will explore most of the viable parameter space in the coming years [4]. Within cosmology, the case in which the Peccei-Quinn symmetry spontaneously breaks after the end of inflation, known as the post-inflationary scenario, is particularly notable for its ability to predict the axion DM abundance. Here however, the axion field develops a distribution with large inhomogeneities on scales set by the horizon at the QCD phase transition, leading to multi-scale dynamics which requires dedicated numerical simulations, see for instance recent works [5–12].

In addition to these complications, it has long been established in the literature [13–16] that, in this scenario, the majority of DM becomes bound into fine-grained, planetary-mass structures known as *miniclusters* (MC), which are too sparsely distributed for direct detection experiments to have a reasonable chance of observing one. Therefore, the feasibility of directly detecting DM axions depends on whether miniclusters survive within our galaxy today. The current understanding of minicluster dynamics relies on a semi-analytic approach that combines initial halo-mass functions from N-body simulations (e.g., [12]) with Monte Carlo modelling of tidal disruption, which is caused by interactions with stellar objects and infall into the galactic halo [17–22]. Despite uncertainties in minicluster properties, the consensus remains that while they may lose a significant portion of their mass,¹ many remnant cores are likely to persist.

In this contribution, we calculate the amount of mass typically stripped from miniclusters, which then contributes to the formation of an ensemble of tidal streams. We ultimately wish to quantify the local axion dark matter distribution in the solar neighborhood and to assess the detectability of axions in the post-inflationary scenario by predicting the typical signal to be observed, see Fig. 1.

2. Disruption of miniclusters

The latest N-body simulations of minicluster formation, starting from the initial conditions left by the collapse of the axion string-wall network during the QCD phase transition [12], provide the initial distribution of masses and density profiles for miniclusters, which are categorised into two types: *merged* minicluster halos and *isolated* miniclusters. Isolated miniclusters are the most abundant by number ($\sim 70\%$), however merged miniclusters comprise most of the DM by mass. With simulation results as input, we model the evolution of miniclusters through the galaxy, focusing on orbits that end in the Solar neighbourhood. Each minicluster orbit will encounter a number of stars along its orbit, depending on the stellar number density of the central bulge and the thin/thick disks, its orbital velocity and a randomly drawn impact parameter. We model stars as point-like objects, and compute the energy injected in each star-minicluster encounter following the distant tide and impulse approximations [23]. For each orbit, mass and radius are updated following the mass loss due to the encounters, and miniclusters are considered completely disrupted only if the sum of all the energy injections exceed their initial binding energy. We find that isolated miniclusters

¹Recent works [21, 22] accounted for the relaxation of the minicluster profile between encounters, demonstrating how the mass loss for each minicluster has been underestimated.

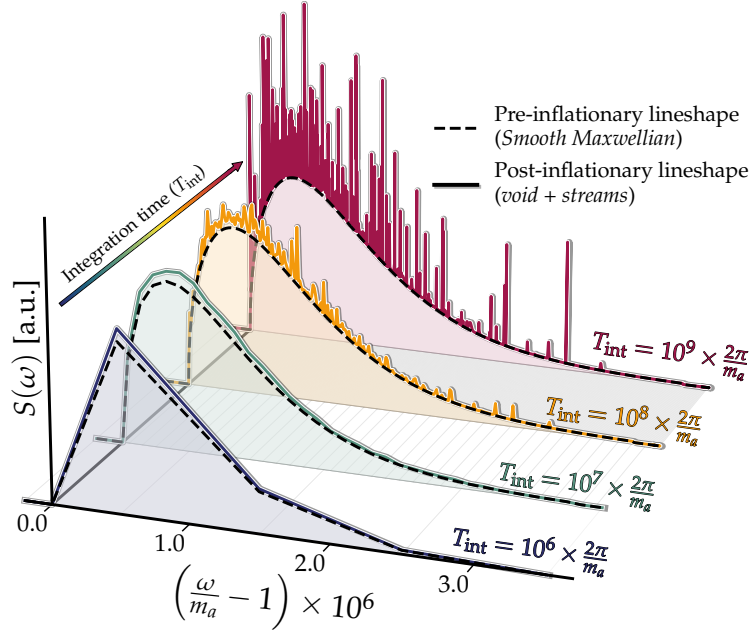


Figure 1: The axion lineshape as a function of the integration time, T_{int} . For long enough exposure, axion haloscopes would have a fine spectral resolution, thereby resolving the streams and distinguishing pre- and post-inflationary axions.

are relatively stable against disruption, however, the high-mass merged miniclusters are much more prone to mass loss, with about half of them losing all of their mass by today. The lost mass which is left unbound is described as a tidal stream of length $\ell_{\text{str}}^i(t) \gtrsim \sigma_{\text{mc}}^i(t - t_{\text{enc}}^i)$, with σ_{mc}^i the MC dispersion velocity at each encounter, the latter happening at a time t_{enc}^i . Furthermore, we simplify the modelling by assuming the stream as a cylinder of the same radius as the original minicluster, and with a Gaussian density profile along the stream length [20]. Numerically, we find streams of length $7.3_{-4.0}^{+3.2}$ pc for merged miniclusters and $0.28_{-0.2}^{+0.34}$ pc for isolated miniclusters.

3. The local axion density

Building on the modeling discussed in the previous section, we outline the expected local density of post-inflationary axions, which consists of three distinct populations:

- *Minivoids.* These axions represent the irreducible background of cold axions, which never cluster into miniclusters. Their overall density is typically $\rho_{\text{void}} \sim 0.1 \rho_{\text{DM}} = 0.045 \text{ GeV/cm}^3$ [11].
- *Cold streams.* Axions in tidal streams are formed from the tidal disruption of the largest and less compact miniclusters. They appear as narrow Gaussian features in the spectral lineshape.
- *Miniclusters.* Axions in the densest halos, which can withstand the tidal forces and that maintain an extremely cold velocity dispersion, $\sigma \sim O(\text{m/s})$. Their occupied volume in the solar neighbourhood is negligible, leading to a rather rare encounter rate.

Results from Monte Carlo simulations of stream formation lead to an expected number $\langle N_{\text{str}} \rangle \simeq \mathcal{O}(10^2 - 10^3)$ of overlapping streams at each point within a local volume $V_{\text{local}} \sim (100 \text{ pc})^3$ [20]. The uncertainty on the estimate accounts for the variations in the density profiles, the concentration of the merged miniclusters, and accounting for additional stream heating [20]. Sampling $\langle N_{\text{str}} \rangle$ streams from our distribution of disrupted miniclusters, we find the energy density stored in all the locally overlapping streams and the background minivoids [20]

$$\rho_a = \rho_{\text{void}} + \sum_{i=1}^{N_{\text{str}}} \rho_{\text{str}}^i \simeq (0.9 \pm 0.06) \rho_{\text{DM}}, \quad (1)$$

where $\rho_{\text{DM}} \approx 0.45 \text{ GeV/cm}^3$ is the DM density that we will use in the following. This represents the main difference between pre- and post-inflationary axions: the overall sensitivity to a certain coupling at fixed signal-to-noise ratio scales as $g_{a\gamma} \propto \rho_a^{-1/2}$, where in the post-inflationary scenario leads to a $\sim 5\%$ suppression with respect to the standard pre-inflationary case.

4. Impact on axion haloscopes

Finally, we can relate the velocity distribution of the streams to the signal (i.e., the lineshape) measured by a typical axion haloscope (see Fig. 1). Field's oscillations are coherent with $\omega = m_a$ until the axion's velocity distribution causes a shift in frequency related to the spread in velocities, happening for integration times close to the axion coherence time $\tau_{\text{coh}} \sim 0.01 \text{ ms} (100 \mu\text{eV}/m_a)$. For integration times $T_{\text{int}} \gg \tau_{\text{coh}}$, the axion's lineshape becomes fully resolved (see also [24, 25]). This resolution allows us to distinguish between a smooth Maxwellian lineshape characteristic of the pre-inflationary scenario, and a series of narrowband Gaussian features corresponding to local post-inflationary streams. Moreover, we find that individual stream features typically persist in the spectral density for approximately $\Delta t = 30_{-11}^{+23}$ years. However, with several hundred to a thousand streams contributing to the lineshape simultaneously, the overall signal variability occurs on much shorter timescales, around tens of days. These time-varying or ultra-narrowband signals are already being targeted by ongoing haloscope experiments using high-resolution adaptations of their standard analysis methods (see, e.g., the recent [26]). Based on our findings, we encourage the continuation and further refinement of these efforts.

Acknowledgements

GP acknowledges support from the Australian Research Council's Discovery Project (DP240103130) scheme. This article is based upon work from COST Action COSMIC WISPerS CA21106, supported by COST (European Cooperation in Science and Technology).

References

- [1] R. D. Peccei and H. R. Quinn, *CP conservation in the presence of instantons*, *Phys. Rev. Lett.* **38** (1977) 1440. [,328(1977)].
- [2] S. Weinberg, *A New Light Boson?*, *Phys. Rev. Lett.* **40** (1978) 223.

- [3] F. Wilczek, *Problem of Strong p and t Invariance in the Presence of Instantons*, *Phys. Rev. Lett.* **40** (1978) 279.
- [4] C. O’Hare, *cajohare/axionlimits: Axionlimits*, <https://cajohare.github.io/AxionLimits/>, July, 2020. 10.5281/zenodo.3932430.
- [5] V. B. . Klaer and G. D. Moore, *The dark-matter axion mass*, *JCAP* **11** (2017) 049 [1708.07521].
- [6] A. Vaquero, J. Redondo and J. Stadler, *Early seeds of axion miniclusters*, *JCAP* **04** (2019) 012 [1809.09241].
- [7] M. Buschmann, J. W. Foster and B. R. Safdi, *Early-Universe Simulations of the Cosmological Axion*, *Phys. Rev. Lett.* **124** (2020) 161103 [1906.00967].
- [8] M. Gorghetto, E. Hardy and G. Villadoro, *More Axions from Strings*, *SciPost Phys.* **10** (2021) 050 [2007.04990].
- [9] C. A. J. O’Hare, G. Pierobon, J. Redondo and Y. Y. Y. Wong, *Simulations of axionlike particles in the postinflationary scenario*, *Phys. Rev. D* **105** (2022) 055025 [2112.05117].
- [10] B. Eggemeier and J. C. Niemeyer, *Formation and mass growth of axion stars in axion miniclusters*, *Phys. Rev. D* **100** (2019) 063528 [1906.01348].
- [11] B. Eggemeier, C. A. J. O’Hare, G. Pierobon, J. Redondo and Y. Y. Y. Wong, *Axion minivoids and implications for direct detection*, *Phys. Rev. D* **107** (2023) 083510 [2212.00560].
- [12] G. Pierobon, J. Redondo, K. Saikawa, A. Vaquero and G. D. Moore, *Miniclusters from axion string simulations*, 2307.09941.
- [13] C. J. Hogan and M. J. Rees, *Axion miniclusters*, *Phys. Lett. B* **205** (1988) 228.
- [14] E. W. Kolb and I. I. Tkachev, *Large amplitude isothermal fluctuations and high density dark matter clumps*, *Phys. Rev. D* **50** (1994) 769 [astro-ph/9403011].
- [15] E. W. Kolb and I. I. Tkachev, *Femtolensing and picolensing by axion miniclusters*, *Astrophys. J. Lett.* **460** (1996) L25 [astro-ph/9510043].
- [16] K. M. Zurek, C. J. Hogan and T. R. Quinn, *Astrophysical Effects of Scalar Dark Matter Miniclusters*, *Phys. Rev. D* **75** (2007) 043511 [astro-ph/0607341].
- [17] B. J. Kavanagh, T. D. P. Edwards, L. Visinelli and C. Weniger, *Stellar disruption of axion miniclusters in the Milky Way*, *Phys. Rev. D* **104** (2021) 063038 [2011.05377].
- [18] V. Dandoy, T. Schwetz and E. Todarello, *A self-consistent wave description of axion miniclusters and their survival in the galaxy*, *JCAP* **09** (2022) 081 [2206.04619].
- [19] X. Shen, H. Xiao, P. F. Hopkins and K. M. Zurek, *Disruption of Dark Matter Minihaloes in the Milky Way environment: Implications for Axion Miniclusters and Early Matter Domination*, 2207.11276.

- [20] C. A. J. O'Hare, G. Pierobon and J. Redondo, *Axion Minicluster Streams in the Solar Neighborhood*, *Phys. Rev. Lett.* **133** (2024) 081001 [[2311.17367](#)].
- [21] I. DSouza, C. Gordon and J. C. Forbes, *Enhanced Disruption of Axion Minihalos by Multiple Stellar Encounters in the Milky Way*, [2411.16166](#).
- [22] I. DSouza and C. Gordon, *Disruption of dark matter minihalos by successive stellar encounters*, *Phys. Rev. D* **109** (2024) 123035 [[2402.03236](#)].
- [23] J. Spitzer, Lyman, *Disruption of Galactic Clusters.*, *Astrophys. J.* **127** (1958) 17.
- [24] J. W. Foster, N. L. Rodd and B. R. Safdi, *Revealing the Dark Matter Halo with Axion Direct Detection*, *Phys. Rev. D* **97** (2018) 123006 [[1711.10489](#)].
- [25] C. A. J. O'Hare and A. M. Green, *Axion astronomy with microwave cavity experiments*, *Phys. Rev. D* **95** (2017) 063017 [[1701.03118](#)].
- [26] ADMX Collaboration, A. T. Hipp et al., *Search for non-virialized axions with 3.3-4.2 μeV mass at selected resolving powers*, [2410.09203](#).